Synthesis of Nanocrystalline TiO_2 and Reduced Titanium Oxides via Rapid and Exothermic Metathesis Reactions

Sujith Perera, Nadiya Zelenski, and Edward G. Gillan*

Department of Chemistry and the Optical Science and Technology Center, University of Iowa, Iowa City, Iowa 52242-1294

Received December 22, 2005. Revised Manuscript Received March 1, 2006

Nanocrystalline titanium dioxide is conventionally produced by aqueous precipitation reactions, followed by annealing post-treatment, which can also cause structural conversions from the photocatalytically active anatase to rutile phases. Solvent-free exothermic solid-state metathesis (SSM) reactions have shown wide utility in the synthesis of binary solids. This paper describes the application and chemical flexibility of the SSM method for the synthesis of TiO_2 from $TiCl_3$ and Na_2O_2. The use of an insulating crucible and addition of a NaCl heat sink to this rapid and exothermic SSM led to improved product crystallinity and increases in anatase to rutile TiO_2 phase content. Small particle size products were synthesized at high salt dilution levels. The photocatalytic activity of SSM synthesized TiO_2 powders containing some anatase TiO_2 were comparable to a commercial TiO_2 standard, even though the SSM powders had 30−50% lower surface areas. By changing the Na_2O_2 reagent to a more oxygen deficient one, Na_2O, reduced titanium phases, primarily Ti_2O_3, were synthesized along with Na−Ti−O structures.

Introduction and Background

The lightest Group 4 dioxide, TiO_2 or titania, has a long and illustrious history as an environmentally stable white pigment and more recently as a light-activated catalytic semiconductor.[1] The two most commonly synthesized titania structures are the low-temperature anatase and high-temperature, thermodynamically stable rutile form. Both of these forms are semiconducting with band gaps of 3.2 and 3.0 eV for anatase and rutile, respectively. Various studies have found that photogenerated electrons and holes promote catalytic processes on the TiO_2 particle surface,[2] possibly aided by transient Ti^{3+} formation.[3] The kinetically stable anatase phase is nearly four times more photocatalytically active than the rutile TiO_2 phase,[4] though mixed phase materials can be more active than pure anatase.[5] One study demonstrated that rutile TiO_2 nanoparticles have significant oxidative catalytic activity,[6] possibly resulting from a large fraction of surface reaction sites.[7] There are intriguing reports on difficult to synthesize anion-doped TiO_2 structures (nitrogen,[8] carbon,[9] and halogens)[10] that are photoactive under the visible light illumination. There is also a recent report that provides strong evidence that oxygen defects formed during different synthetic preparations also enhance TiO_2 visible light absorption.[11]

The synthesis of TiO_2 materials generally falls into vapor phase or solution phase categories. The former method is demonstrated by $TiCl_4$ vapor hydrolysis to produce high surface area commercial materials, such as Degussa's P25 TiO_2 (∼4:1 anatase/rutile), which is often a benchmark standard in photocatalytic studies. Vapor phase $TiCl_4$ is also used to deposit TiO_2 films.[12] Bulk metal oxide powders are conventionally produced via aqueous condensation and precipitation methods,[13] though such methods for TiO_2 synthesis usually result in poorly ordered materials that crystallize to anatase TiO_2 when thermal treatments are below ∼500 °C. At higher temperatures, anatase irreversibly

* To whom correspondence should be addressed. E-mail: edward-gillan@uiowa.edu.

(1) Wold, A. *Chem. Mater.* **1993**, *5*, 280.
(2) (a) Linsebigler, A. L.; Lu, G.; Yates, J. T., Jr. *Chem. Rev.* **1995**, *95*, 735 and references therein. (b) Carp, O.; Huisman, C. L.; Reller, A. *Prog. Solid State Chem.* **2004**, *32*, 33 and references therein. (c) Konstantinou, I. K.; Albanis, T. A. *Appl. Catal. B* **2004**, *49*, 1.
(3) (a) Anpo, M.; Takeuchi, M. *J. Catal.* **2003**, *216*, 505. (b) Indris, S.; Amade, R.; Heitjans, P.; Finger, M.; Haeger, A.; Hess, D.; Grunert, W.; Borger, A.; Becker, K. D. *J. Phys. Chem. B* **2005**, *109*, 23274.
(4) (a) Tanaka, K.; Capule, M. F. V.; Hisanaga, T. *Chem. Phys. Lett.* **1991**, *187*, 73. (b) Ding, Z.; Lu, G. Q.; Greenfield, P. F. *J. Phys. Chem. B* **2000**, *104*, 4815.
(5) Kawahara, T.; Konishi, Y. Tada, H.; Tohge, N.; Nishii, J.; Ito, S. *Angew. Chem., Int. Ed.* **2002**, *41*, 2811.
(6) Yin, H.; Wada, Y.; Kitamura, T.; Kambe, S.; Murasawa, S.; Mori, H.; Sakata, T.; Yanagida, S. *J. Mater. Chem.* **2001**, *11*, 1694.
(7) Ferretto, L.; Glisenti, A. *Chem. Mater.* **2003**, *15*, 1181.
(8) (a) Asahi, R.; Morikawa, T.; Ohwaki, T.; Aoki, K.; Taga, Y. *Science* **2001**, *393*, 269. (b) Kahn, S. U. M.; Al-Shahry, M.; Ingler, W. B., Jr. *Science* **2002**, *297*, 2243. (c) Burda, C.; Lou, Y.; Chen, X.; Samia, A. C. S.; Stout, J.; Gole, J. L. *Nano Lett.* **2003**, *3*, 1049. (d) Gole, J. L.; Stout, J. D.; Burda, C.; Lou, Y.; Chen, X. *J. Phys. Chem.* **2004**, *108*, 1230. (e) Diwald, O.; Thompson, T. L.; Zubkov, T.; Goralski, E. G.; Walck, S. D.; Yates, J. T., Jr. *J. Phys. Chem. B* **2004**, *108*, 6004.
(9) Sakthivel, S.; Kisch, H. *Angew. Chem., Int. Ed.* **2003**, *42*, 4908.
(10) (a) Hong, X.; Wang, Z.; Cai, W.; Lu, F.; Zhang, J.; Yang, Y.; Ma, N.; Liu, Y. **2005**, *17*, 1548. (b) Li, D.; Haneda, H.; Labhsetwar, N. K.; Hishita, S.; Ohasi, N. *Chem. Phys. Lett.* **2005**, *401*, 579.
(11) Martyanov, I. N.; Uma, S.; Rodriques, S.; Klabunde, K. J. *Chem. Commun.* **2004**, 2476.
(12) (a) O'Neill, S. A.; Parkin, I. P.; Clark, R. J. H.; Mills, A.; Elliott, N. *J. Mater. Chem.* **2003**, 13, 56 and references therein. (b) O'Neill, S. A.; Clark, R. J. H.; Parkin, I. P. *Chem. Mater.* **2003**, *15*, 46.
(13) (a) Matijevic, E. *Chem. Mater.* **1993**, *5*, 412 and references therein. (b) Brinker, C. J.; Scherer, G. W. *Sol Gel Science*; Academic Press: New York, 1990. (c) Sanchez, C.; Livage, J. *New J. Chem.* **1990**, *14*, 513. (d) Barbe, C. H.; Arendse, F.; Comte, P.; Jirousek, M.; Lenzmann, F.; Shklover, V.; Gratzel, M. *J. Am. Ceram. Soc.* **1997**, *80*, 3157. (e) Kotov, N. A.; Meldrum, F. C.; Fendler, J. H., *J. Phys. Chem.* **1994**, *98*, 8827. (f) Tang, J.; Redl, F.; Zhu, Y.; Siegrist, T.; Brus, L. E.; Steigerwald, M. L. *Nano Lett.* **2005**, *5*, 543.

10.1021/cm0528328 CCC: $33.50
Published on Web 03/30/2006

converts to the rutile. Several studies that have synthesized nanocrystalline anatase in solution without thermal post-treatments.[14]

An alternative solid-state synthetic method termed solid-state metathesis (SSM) synthesis uses rapid exothermically driven reaction processes that have some degree of precursor flexibility and reaction control. SSM reactions utilize metal halides (MX_y) reacted with an alkali metal or alkaline earth metal component (e.g., Na_2S, Na_3P, MgB_2, Li_3N) to produce crystalline metal sulfides, phosphides, borides, and nitrides.[15] Highly exothermic and self-propagating SSM reactions usually release sufficient energy to melt the halide salt byproduct ($T > 1000$ °C). They are briefly analogous to flux-assisted solid-state syntheses and crystallization methodologies[16] but have a short window for significant atom diffusion and crystallization to occur (usually < 5 s).

The SSM reaction methodology has also shown utility in the synthesis of simple metal oxides (e.g., ZrO_2, Cr_2O_3), mixed metal oxide systems (e.g., $LaFeO_3$, Li_2TiO_3),[17] and metal-doped cubic stabilized ZrO_2 structures.[18] Because SSM reactions often reach very high transient temperatures (~1300 °C), they usually produce thermodynamically stable metal oxides. Attempts at producing metastable crystalline solids have generally eluded researchers utilizing exothermic SSM reactions. One way to moderate temperatures in these reactive and exothermic systems is to use an external component to absorb heat and dilute the precursor mixture. A nonaqueous solvent environment can serve in this regard,[19] but in a traditional SSM reaction this is most easily accomplished by adding excess byproduct alkali halide (e.g., NaCl) to the reaction. This inert heat-absorbing additive will increase the amount of molten salt, which can aid in crystallization of disordered metal oxides and improve reagent mixing and atom diffusion. Salt additives for internal temperature control have been used to reduce product particle size in SSM reactions.[20] Less energetic metathesis reactions have also been effectively used to create macroporous complex magnetic metal oxide structures.[21]

In the current study, we describe a SSM method to rapidly synthesize nanocrystalline rutile TiO_2 and, under salt-moderated reaction conditions, to produce intimately mixed rutile/anatase TiO_2 materials. The degree of salt addition influences the amount of anatase and the particle size of the TiO_2 product. The photocatalytic abilities of various nanocrystalline titania products were examined by aqueous UV light promoted degradation of an organic dye. With a simple change in the solid oxide SSM precursor from Na_2O_2 to more oxygen-poor Na_2O, mixed phase reduced titanium oxides and Na_xTiO_y structures are formed. The wide flexibility of the SSM approach makes it likely that the syntheses described below can be modified to produce other more complex metastable metal oxides.

Experimental Section

Solid-State Titanium Oxide Metathesis Reactions. All solvents and reagents were used as received. The following reagents were used for the synthesis of titanium oxides, specifically using $TiCl_3$ for TiO_2 [$TiCl_3$ (1.00 g, 6.48 mmol, Aldrich, 99%) and Na_2O_2 (0.758 g, 9.72 mmol, Alfa Aesar, 93% min)] and for Ti_2O_3 [$TiCl_3$ (1.00 g, 6.48 mmol) and Na_2O (0.602 g, 9.71 mmol, Aldrich, 97%)]. The molar ratio of $TiCl_3$ to Na_2O_x is 1 to 1.5 to ensure that all sodium and chlorine could ideally be sequestered as NaCl in the product. In the reactions that targeted Na_xTiO_y phases, 6.48 mmol of $TiCl_3$ and either 10.50 or 11.29 mmol of Na_2O was used. The solid reagent powders were ground together with a mortar and pestle in an argon-filled glovebox (Vacuum Atmospheres MO-40M) and put into a 60-mL custom-built calorimeter-style steel reactor that was described in previous work (screw top, inner dimensions of 5 cm depth × 3.8 cm width, 5 mm thick walls, and a removable steel cap with four insulated posts).[22] Reactions were performed with and without a ceramic crucible powder container (15 mL, Coors no. 60105). Two posts on the reactor lid were fitted with a Nichrome filament that was buried a few millimeters into the pile of reactant powder. The closed reactor was removed from the glovebox, and the filament was resistively heated (~2 s, 10−20 V direct current) to produce local heating (ca. 700 °C) that initiated a self-sustaining metathesis reaction. *Safety note: SSM reactions have been known to initiate upon grinding solid reagents together, so care should be taken whenever investigating a new reactant pairing. For example, the $TiCl_3/Na_2O$ reaction will initiate with a red-hot flash if it is vigorously ground for ~10 min with a mortar and pestle. Reactions should be performed on small scales in reactors with pressure release options.*

After the completed SSM reaction had cooled to room temperature, the reactor was opened in air, and the solid product was ground to a fine powder with a mortar and pestle and stirred in 1 M HCl (~80 mL for 1 g of as-synthesized product) for 15−30 min to remove any unreacted starting materials, NaCl byproducts, and any soluble side products. The washed solid was isolated using vacuum filtration, rinsed with several aliquots of distilled water to ensure that all traces of NaCl were removed, and then dried in a 140 °C oven in air for ~10 min.

In salt heat sink studies, the 6.48 mmol of $TiCl_3$ and 9.72 mmol of Na_2O_2 or Na_2O were ground together in the glovebox, and then NaCl powder (1.5−4 g, ~25−70 mmol, EM Science) was ground with this precursor mixture. The salt-diluted mixture was placed in the ceramic crucible or directly into the steel reactor and initiated as described above. Because of diluent effects, a coiled ignition wire was used for mixtures with greater than 3 g of NaCl/g of $TiCl_3$. These salt addition reactions could still be initiated with a straight heated wire, but occasionally propagation was incomplete and yields were low (~20%). The coiled filament was formed by wrapping 10 loops of a 24 gauge (~0.5 mm) Nichrome wire around a 2 mm diameter rod. Reactions initiated using this coiled wire produced

(14) (a) Niederberger, M.; Bartl, M. H.; Stucky, G. D. *Chem. Mater.* **2002**, *14*, 4364. (b) Daoud, W. A.; Xin, J. H. *Chem. Commun.* **2005**, 2110.
(15) (a) Parkin, I. P. *Transition Met. Chem.* **2002**, *27*, 569. (b) Gillan, E. G.; Kaner, R. B. *Chem. Mater.* **1996**, *8*, 333. (c) Parkin, I. P. *Chem. Soc. Rev.* **1996**, 199.
(16) Elwell, D.; Scheel, H. J. *Crystal growth from high-temperature solutions*; Academic Press: New York, 1975.
(17) (a) Hector, A.; Parkin, I. P. *Polyhedron* **1993**, *12*, 1855. (b) Wiley, J. B.; Gillan, E. G.; Kaner, R. B. *Mater. Res. Bull.* **1993**, *28*, 893. (c) Parkin, I. P.; Komarov, A. V.; Fang, Q. *Polyhedron* **1996**, *15*, 3117. (d) Aguas, M. D.; Combe, G. C.; Parkin, I. P. *Polyhedron* **1998**, *17*, 49.
(18) Gillan, E. G.; Kaner, R. B. *J. Mater. Chem.* **2001**, *11*, 1951.
(19) (a) Grocholl, L.; Wang, J.; Gillan, E. G. *Chem. Mater.* **2001**, *13*, 4290. (b) Hu, J.; Lu, Q.; Tang, K.; Yu, S.; Qian, Y.; Zhou, G.; Liu, X. *J. Am. Ceram. Soc.* **2000**, *83*, 430.
(20) (a) Jarvis, R. F., Jr.; Jacubinas, R. M.; Kaner, R. B. *Inorg. Chem.* **2000**, *39*, 3243. (b) Janes, R. A.; Aldissi, M.; Kaner, R. B. *Chem. Mater.* **2003**, *15*, 4431.
(21) Toberer, E. S.; Weaver, J. C.; Ramesha, K.; Seshadri, R. *Chem. Mater.* **2004**, *16*, 2194.
(22) Miller, D. R.; Wang, J.; Gillan, E. G. *J. Mater. Chem.* **2002**, *12*, 2463.

more reproducible and homogeneous propagation and higher isolated yields.

Selected as-synthesized and washed products were annealed at elevated temperatures (400−1000 °C) in air or in sealed, evacuated silica ampules for 1−2 days. These annealing studies were performed to investigate the thermal stability of the phase, composition, and morphology of as-synthesized titanium oxides.

Characterization of Titanium Oxide Metathesis Reaction Products. The phase and crystallinity of the products were analyzed by powder X-ray diffraction (XRD) using a Siemens D5000 diffractometer (50 kW, 30 mA, 0.03°/step, and 3−6 s/step count times). Phase identification was made using reference data from the JCPDS database. A crystalline silicon powder external standard consisting of a finely ground single-crystal silicon wafer (>99.9%) was used as a reference for crystallite size measurements. The titanium oxide product's average crystallite sizes were calculated from peaks in the 20−30° 2θ region using the Scherrer and Warren equations.[23] Relative amounts of the anatase and rutile phases were calculated using the intensities of their most intense XRD peaks near 25.5° and 27.5°, respectively, and an empirical relationship developed by Spurr and Myers.[24] Infrared spectra were taken on a Nicolet Nexus 670 spectrometer in transmission mode using KBr pellets containing dilute products. Thermogravimetric−differential thermal analysis (TG-DTA) experiments were performed on a Seiko Exstar 6300 TG/DTA system under flowing argon or dry air with a 5−10 °C/min heating ramp. Metal contents for Ti_2O_3 were determined thermogravimetrically by oxidizing it to TiO_2 at elevated temperatures. Scanning electron microscopy (SEM) information was obtained with a Hitachi S-4000 field emission system (5 kV) on powders affixed to aluminum holders with carbon tape. This system includes an IXRF X-ray microanalysis system for energy dispersive spectroscopy (EDS; 20 kV) that provided semiquantitative information on relative amounts of titanium, sodium, and chlorine in the samples. The surface area was determined by nitrogen adsorption isotherms and BET calculations using a Nova 1200 Quantachrome analyzer.

Dye Photodegradation by Titanium Oxide Powders. The ultraviolet photochemical activity of SSM synthesized titanium oxide powders was determined using broad spectrum UV light exposure (ACE-Hanovia 450 W high-pressure mercury lamp, Pyrex water jacket) in the presence of methylene blue (MB) aqueous solutions (3.033×10^{-5} M or 0.0114 g/L in 18 MΩ distilled water). Initially, closed glass vials containing 10 mg of TiO_x powder and 10 mL of the MB solution were stirred in the dark for various times (5−30 min) to measure the amount of dye surface adsorption as determined by stable MB solution concentrations. The titania powders reached stable dark MB adsorption values after 20 min, and each sample in this study was incubated with the MB solution for this length of time before UV exposure studies. After dark equilibration, the vials were then opened and stirred under UV lamp illumination for 5 min intervals. The suspensions were then centrifuged, and the solution MB concentration was determined by measuring the intensity of the MB absorption peak in the 643−664 nm region relative to the background level at 750 nm using an HP 8453 UV−vis absorption spectrometer (190−1100 nm range, 1 nm resolution). The decrease in the intensity of the absorption band in the ~650 nm region was used as an indication of dye oxidation on the TiO_2 particle surface.[25] The percent MB remaining in solution was referenced to the absorbance of the MB standard solution prior to irradiation. The measured solutions were returned to the original vial for subsequent irradiation experiments. For comparison, commercial TiO_2 (Degussa P25, 99.5%, mixture of anatase and rutile) was washed in the same manner as that used for SSM TiO_2 powders to produce comparable initial surface properties and analyzed under the same photochemical conditions.

Results and Discussion

Rapid Synthesis of Crystalline TiO_2 from a SSM Reaction. The basic requirement that must be fulfilled for a successful rapid SSM (exchange) reaction is that a thermodynamic driving force must exist for the reaction to proceed with no sustained external energy. In the current study, the production of an alkali halide salt, NaCl, provides the enthalpic drive for the transformation of $TiCl_3$ to Ti(III) or Ti(IV) oxide or peroxide intermediates that quickly condense to extended Ti−O structures. The ideal balanced reaction of $TiCl_3$ with Na_2O_2 is shown in eq 1.

$$TiCl_3 + 1.5Na_2O_2 \rightarrow \mathbf{TiO_2} + 3NaCl + 0.5O_2 \qquad (1)$$

After a heated filament initiated a self-sustaining reaction between $TiCl_3$ and Na_2O_2, the reactor's steel walls became hot to the touch and a white vapor evolved from under the reactor's lid. The metal walls quickly dissipated the reaction's evolved heat and cooled the system below the NaCl melting point, resulting in mainly a fused yellow-tan product mass at the bottom of the reactor with about a third of the solid splattered on the walls. The XRD pattern of the as-synthesized solid is dominated by crystalline NaCl peaks along with small rutile TiO_2 peaks. After washing away the NaCl byproduct, the remaining off-white solid has an XRD pattern consistent with the thermodynamically stable high-temperature rutile TiO_2 structure (Figure 1a, primitive tetragonal structure, JCPDS no. 21-1276). The solid IR data for the washed product is also consistent with Ti−O lattice vibrations (530 and 660 cm^{-1}) and surface bound OH groups generated during washing (~1600 and 3400 cm^{-1}).[26]

While the isolated yields in this SSM TiO_2 synthesis are respectable (50%, see Table 1), the dilute acid wash is critical to limit contamination from sodium containing side products that can form during the exothermic reaction. For example, XRD data on water-washed products that were subsequently annealed at 1000 °C showed clear evidence of secondary phases such as $Na_2Ti_6O_{13}$ ($Na_2O-6TiO_2$ or $Na_{0.33}TiO_{2.17}$, JCPDS no. 37-0951). Because $TiCl_3$ decomposes to $TiCl_2$(s) and $TiCl_4$(g) near 450 °C,[27] gas-phase loss of some titanium reagent will lower yields and leave excess Na_2O_2 that could engage in further reactions with as-formed TiO_2. EDS on the acid-washed TiO_2 shows that sodium levels are typically less than 3.5 mol % relative to titanium (i.e., Na/Ti < 0.035) and chlorine levels are below detection limits (<1 mol %). Note that related sealed tube metathesis reactions using Li_2O

(23) Warren, B. E. *X-ray Diffraction*; Dover Publications: New York, 1990; pp 251−258.
(24) Spurr, R. A.; Myers, H. *Anal. Chem.* **1957**, *29*, 760.
(25) (a) Xu, N.; Shi, Z.; Fan, Y.; Dong, J.; Shi, J.; Hu, M. Z.-C. *Ind. Eng. Chem. Res.* **1999**, *38*, 373. (b) Houas, A.; Lachheb, H.; Ksibi, M.; Elaloui, E.; Guillard, C.; Herrmann, J.-M. *Appl. Catal. B* **2001**, *21*, 145.
(26) NIST Chemistry WebBook. http://webbook.nist.gov/ (accessed June 2006).
(27) (a) Schumb, W. C.; Sundstrom, R. F. *J. Am. Chem. Soc.* **1933**, *55*, 596. (b) Altman, D.; Farber, M.; Mason, D. M. *J. Chem. Phys.* **1956**, *25*, 531.

Table 1. Synthetic and Structural Data for SSM Titanium Oxide Products

reagents[a]	mol of NaCl/ mol of $TiCl_3$	yield[b] (%)	TiO_2 phase ratio (rutile:anatase)	crystallite size rutile:anatase (nm)	IR (cm^{-1})	T_{max}, °C (% NaCl melts)	surface area (m^2/g)
$TiCl_3/Na_2O_2$, no crucible	0	50	100:0	72 (rutile)	528, 666	1465	6.6
$TiCl_3/Na_2O_2$	0	42	100:0	76 (rutile)	528, 665	1465	2.6
$TiCl_3/Na_2O_2$	5.3	67	90:10	68:27	507, 603	908	13
$TiCl_3/Na_2O_2$	7.9	58	73:27	54:27	574, 524	801 (67)	15
$TiCl_3/Na_2O_2$	9.2	57	61:39	60:27	527 (br)	801 (45)	27
$TiCl_3/Na_2O_2$	10.6	47	46:54	57:25	520 (br)	801 (26)	23

[a] Reactions were performed using a ceramic crucible insert in a steel reactor unless noted otherwise. [b] The yield was calculated based on TiO_2 after washing away NaCl.

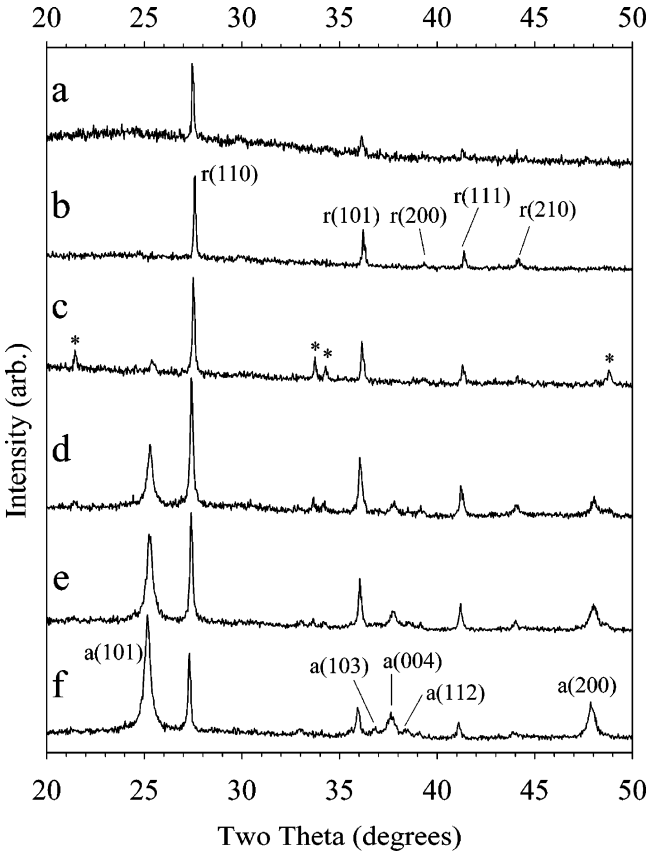

Figure 1. XRD stack plot of TiO_2 produced from the SSM reaction between $TiCl_3$ and $1.5Na_2O_2$ (a) performed directly in the metal reactor, (b) using a crucible insert, and in a crucible with an additional (c) 5.3 mol of NaCl/ mol of $TiCl_3$, (d) 7.9 mol of NaCl/mol of $TiCl_3$, (e) 9.2 mol of NaCl/mol of $TiCl_3$, and (f) 10.6 mol of NaCl/mol of $TiCl_3$. Miller indices labels for rutile peaks are noted with r(*hkl*) labels, and anatase peaks are noted with a(*hkl*) labels. The * denotes a Ti_3O_5 phase.

also produced crystalline rutile TiO_2 and could be intentionally driven to Li_2TiO_3 products.[17a,d]

Effect of SSM Reaction Containment on TiO_2 Products. To compare the effect of cooling rate on product phase and crystallinity, a ceramic crucible was used to insulate the solid reagents from the metal reactor walls. An insulating ceramic cup has shown some reaction influence in other SSM systems.[28] When a $TiCl_3/Na_2O_2$ mixture was placed in a ceramic crucible inside the steel reactor, it initiated easily and produced TiO_2 that was qualitatively similar to reactions performed directly in the metal reactor (Figure 1b) but with more well-resolved XRD peaks at high 2θ angles. In addition, most of the product remained inside the crucible as a cohesive mass for easy recovery. There was also a longer retention of heat by the crucible compared to the reaction in contact with the metal walls. The average TiO_2 crystallite size is slightly larger when the crucible is used, but both are less than 80 nm (Table 1). The latter effect can be explained by a better contained molten salt post-reaction flux that improves ordering in the formed nanocrystallites. The slightly lower yields with the crucible may result from a hotter reaction zone that could facilitate more $TiCl_3$ decomposition to $TiCl_4$ gas, which would remove titanium precursor components from the reactive melt and lower the overall product yields.

Controlling SSM Reaction Energetics and TiO_2 Phase Using an NaCl Heat Sink. SSM reactions have been recognized as approximately adiabatic in nature, because they occur so rapidly that all of the released enthalpy is essentially used to heat up the solid and liquid products, usually raising the alkali halide near or above its normal boiling point.[15] The number of moles of NaCl, to a great extent, dictates the overall exothermicity of many SSM reactions (e.g., ΔH_f of NaCl = −386 kJ/mol), but it also limits the maximum reaction temperature (T_{max}) because it absorbs heat to melt and rise in temperature based on its heat capacity. By considering the product heats of transition and heat capacities, an ideal T_{max} value is determined as the point where all of the heat of reaction is expended to raise the temperature of the products.[16] In the present case, the eq 1 reaction is exothermic (ΔH_{rxn} = −687 kJ/mol of Ti) and has a T_{max} of 1465 °C, which is the boiling point of NaCl, and there is sufficient energy to evaporate 46% of the NaCl byproduct.

The reaction in eq 1 was performed with varying amounts of NaCl that acts as an internal heat sink (eq 2) and will alter T_{max} and the amount of molten salt flux that is formed during the rapid SSM TiO_2 reaction.

$$TiCl_3 + 1.5\,Na_2O_2 + x\mathrm{NaCl} \rightarrow \mathbf{TiO_2} + (3 + x)\mathrm{NaCl} + 0.5O_2 \quad (2)$$

The ceramic crucible holder was used to keep the products in more of a compact and intimate environment and improve the crystallinity of as-synthesized materials in a larger molten salt flux. The $TiCl_3/Na_2O_2$ reagents were intimately ground together and then mixed with the excess NaCl. After initiation and cooling, the product was a dense cement-like mass in the bottom of the ceramic cup. As the amount of added NaCl was increased, the degree of homogeneous propagation decreased; thus, a coiled initiation filament was needed for NaCl additions of $x \geq 7.9$ (see Experimental Section). XRD scans of the washed products show clear evidence for the low-temperature, metastable anatase TiO_2

(28) Janes, R. A.; Low, M. A.; Kaner, R. B. *Inorg. Chem.* **2003**, *42*, 2714.

(body-centered tetragonal, JCPDS no. 21-1272) for $x = 5.3-10.6$ (2−4 g of NaCl/g of $TiCl_3$, see Figure 1c−f). As noted in Figure 1, a reduced titanium oxide component appears at $x = 5.3$ that is most closely associated with a Ti_3O_5 XRD pattern ($TiO_{1.67}$, JCPDS no. 11-0217). After briefly heating this sample in air at 500 °C, these impurity peaks vanish and the anatase peaks are more prominent, supporting the contention that the impurity peaks correspond to an oxygen-deficient Ti−O phase.

The NaCl dilutions clearly result in an increase in the anatase to rutile phase ratio, but surprisingly, yields and TiO_2 crystallinity were essentially unchanged, even at the highest NaCl dilution levels ($x = 10.6$). Table 1 lists chemical yields based on TiO_2 and crystallite sizes and relative anatase to rutile contents based on an analysis of XRD peak widths and intensities. The XRD data show that smaller crystallite sizes are observed for the anatase phase versus the rutile phase. This is consistent with results from previous annealing studies on precipitated TiO_2 that observe irreversible anatase to rutile transformations as the anatase crystallite size grows above ∼15 nm.[29]

Sluggish or failed SSM propagation has been previously observed if the maximum reaction temperature is below a minimum temperature, which is usually near the decomposition/phase transition point of one reagent.[15] Propagation problems also occur when the precursors are too diluted to locally expel enough energy to melt the surrounding matrix. In the current study, the $TiCl_3 \rightarrow TiCl_2 + TiCl_4$ transition near 450 °C likely represents the minimum propagation temperature, consistent with observations in other SSM studies using $TiCl_3$.[20b,30] Even at the highest NaCl additions used here, the calculated T_{max} values do not drop below the NaCl melting point (801 °C) and thus all reactions readily propagate and generate a transient molten salt flux (Table 1). The reaction using 10.6 mol of added NaCl/mol of $TiCl_3$ releases barely enough heat to reach the NaCl melting point and less than one-third of the NaCl is melted. The isolated yields in Table 1 are not significantly affected by the salt additions, and they may actually be improved by the increase in molten flux that cools the overall reaction, decreases the amount of $TiCl_3$ decomposition, and limits reaction splatter in the crucible.

The ceramic crucible is very important in aiding in the flux-assisted growth of crystalline anatase TiO_2 from the SSM reaction shown in eq 2. When salt additions were performed without the insulating crucible, reactions for $x > 4$ (1.5 g of NaCl/g of $TiCl_3$) only partially propagate. For $x < 4$ salt additions, the only crystalline product is rutile, though an amorphous Ti−O component is present that crystallizes to anatase upon heating in air at 500 °C. Taken as a whole, the above data indicate that the added salt and the crucible produce a longer lived molten NaCl flux in the crucible that aids in product crystallization, in addition to drawing enthalpy from the overall reaction, which increases the survival of an anatase phase component. Without the crucible, the added salt combines with heat removal by the metal reactor walls and cools the reaction below the point where it can propagate and effectively generate a flux to assist in product crystallization.

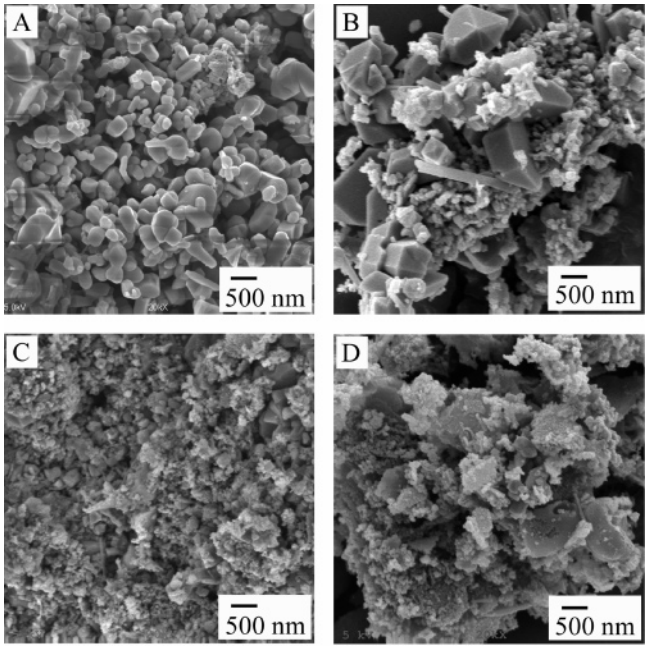

Figure 2. SEM images of the washed SSM TiO_2 reaction products synthesized (A) without added NaCl and in a crucible with an additional (B) 5.3 mol of NaCl/mol of $TiCl_3$, (C) 7.9 mol of NaCl/mol of $TiCl_3$, and (D) 10.6 mol of NaCl/mol of $TiCl_3$.

TiO_2 Morphologies with and without NaCl Additions. From the XRD data shown in Table 1, one observes that the crystallite sizes decrease slightly with added NaCl content, though not uniformly. While the molten salt flux may act as an efficient crystallization medium, its diluent capabilities should also limit particle size growth; thus, the products were examined by SEM. A SEM image of the TiO_2 product with no salt added shows aggregated particles with relatively smooth edges in submicrometer sizes near 500 nm (Figure 2A). When 5.3 mol of additional NaCl/mol of $TiCl_3$ and a crucible are used, the product contains several well-faceted micrometer-sized crystallites combined with smaller elongated structures interspersed with submicrometer particles (Figure 2B). With higher NaCl additions, the particle shape gradually shrinks and becomes less faceted, finally leading to finely dispersed ∼100 nm particles (Figure 2C,D). The TiO_2 products for $x > 7.9$ have morphologies reminiscent of the commercial Degussa P25 TiO_2 standard. At $x = 10.6$, larger aggregates are generated as the small ∼50 nm particles stick together.

Molten alkali halide salts have a long history as a crystal growth medium; however, in the current study this is balanced with the short-lived nature of such a melt. On a short time scale, the molten NaCl may dissolve $TiCl_x$ species and Na_2O_2 and facilitate their reaction and TiO_2 crystallization. Note that growing TiO_2 nuclei are embedded in a 3- to 13-fold excess of molten NaCl; thus, they are diluted and kept apart at high NaCl contents. The cooling and diluent character of the excess NaCl likely contributes to the decrease in TiO_2 particle sizes by limiting product diffusion and growth. This cooling effect from the salt heat sink also promotes the production of the low-temperature anatase TiO_2

(29) Zhang, H.; Banfield, J. F. *J. Mater. Chem.*, **1998**, *8*, 2073.
(30) Blair, R. G.; Gillan, E. G.; Nguyen, N. K. B.; Daurio, D.; Kaner, R. B. *Chem. Mater.* **2003**, *15*, 3286.

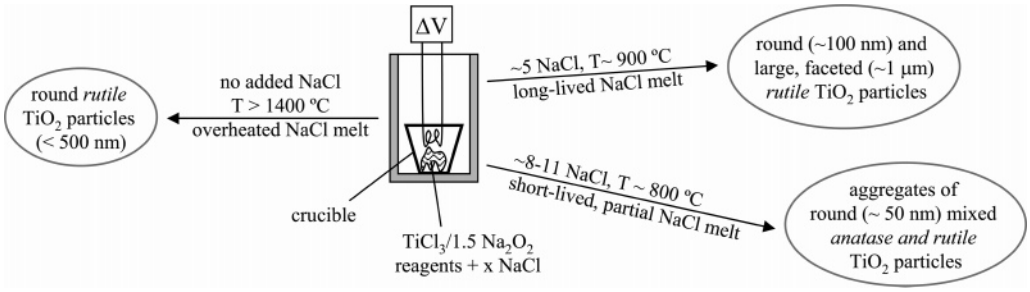

Figure 3. SSM reactor schematic and resulting TiO_2 products with different NaCl additions to the reaction between $TiCl_3$ and $1.5Na_2O_2$.

phase, which usually converts to rutile upon extended heating above ~500 °C. A cartoon schematic of the SSM reactor and the overall effect of NaCl on the crystal phase and particle size is shown in Figure 3.

UV Photocatalytic Properties of SSM Generated Titanias. As noted in Introduction, TiO_2 has well-established UV photocatalytic abilities, mostly related to organic oxidative degradation reactions.[31] The photooxidation of MB dye solutions in the presence of various SSM synthesized titanium oxides was examined and compared with the activity of a commercial mixture of anatase and rutile (Degussa P25, 81% anatase based on XRD analysis). The acid-washed TiO_2 SSM reaction products noticeably adsorbed a higher percentage of the dye solution than the P25 material under dark conditions ranging from ~15 to 60% of the MB in solution. Generally SSM products with the higher rutile content adsorbed more MB from solution, and all SSM TiO_2 samples adsorbed a larger amount of MB than the P25 standard even though its surface area (54 m^2/g) is greater than all SSM samples (Table 1). Previous studies have shown that subtle variations in TiO_2 surface acidity lead to large differences in the amount of adsorbed MB on the oxide surface,[32] and other work has shown that the amount of MB adsorbed on TiO_2 does not easily correlate with surface area.[25a] Because the SSM TiO_2 originated from a Ti^{3+} and peroxide precursor, the surface may contain residual Ti^{3+} sites,[3b] which could produce a less acidic surface than that of the P25 and make the SSM TiO_2 more attractive to the dissolved cationic MB species. We are currently utilizing surface and electron paramagnetic resonance analysis to determine whether such subtle surface site differences are present in the SSM TiO_2 powders.

Figure 4 plots the solution MB content (relative to an MB standard solution) as a function of sequential UV irradiation in the presence of SSM TiO_2 samples synthesized with varying amounts of NaCl.[25] Data for an acid-washed Degussa P25 sample is also plotted for comparison. After 15 min of UV exposure, the SSM products developed a pale purple/violet surface color versus the P25 TiO_2, which remained white. This violet surface-adsorbed species was observed by others and determined to be a partial oxidation product of MB, where its terminal *N*-methyl groups are demethylated to amines, leading to a thionine dye intermediate that appears violet.[32] Successive UV irradiation and analysis showed that the SSM synthesized rutile TiO_2 is less photochemically

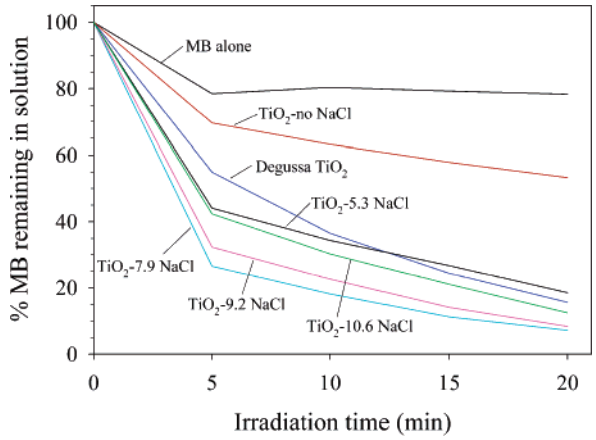

Figure 4. UV photodegradation of MB in the presence of several TiO_2 samples produced from the SSM reaction between $TiCl_3$ and $1.5Na_2O_2$ plotted relative to absorption of a standard MB solution. Noted NaCl values refer to excess moles of NaCl/mol of $TiCl_3$ added to the reaction.

active on a weight basis than the P25 TiO_2 standard. For reference, rutile TiO_2 shows, at best, ~20% of the organic photooxidation rate as compared to anatase TiO_2.[4] It is significant that SSM TiO_2 photoactivity increases with NaCl additions, which corresponds to larger anatase product content and generally smaller particle sizes; thus, diluent/heat sink effects are also evident in solution photocatalytic abilities. The photocatalytic decomposition of MB for $x = 7.9$ and 9.2 NaCl SSM samples is more rapid than that of P25 TiO_2, though their surface area is 50−70% lower than P25.

SSM Synthesis of Reduced Titanium Oxides. One additional advantage with the reaction shown in eq 1 is that there are other available Na−O solid reagents with different Na/O ratios that can potentially allow access to lower oxidation state TiO_x materials. Equation 3 details how $TiCl_3$ reacted with Na_2O should produce Ti_2O_3, which contains Ti(III) versus Ti(IV) in TiO_2; thus, the precursor's titanium oxidation state should be preserved in the oxygen deficient SSM reaction environment.

$$TiCl_3 + 1.5Na_2O \rightarrow 0.5\mathbf{Ti_2O_3} + 3NaCl \qquad (3)$$

The exothermic SSM reaction shown in eq 3 ($\Delta H_{rxn} = -645$ kJ/mol of Ti) rapidly proceeds upon filament initiation and yields a black product containing crystalline NaCl as detected by XRD. The presence of poorly crystalline Ti_2O_3 ($TiO_{1.5}$, rhombohedral, Al_2O_3 structure type, JCPDS no. 43-1033) in the black washed product was verified by XRD (Figure 5a). A few smaller peaks can be attributed to Ti_3O_5, which could form if some of the titanium reagent volatilized from

(31) Konstantinou, I. K.; Albanis, T. *A. Appl. Catal. B* **2004**, *49*, 1.
(32) Zhang, T.; Oyama, T.; Aoshima, A.; Hidaka, H.; Zhao, J.; Serpone, N. *J. Photochem. Photobiol., A* **2001**, *140*, 163.

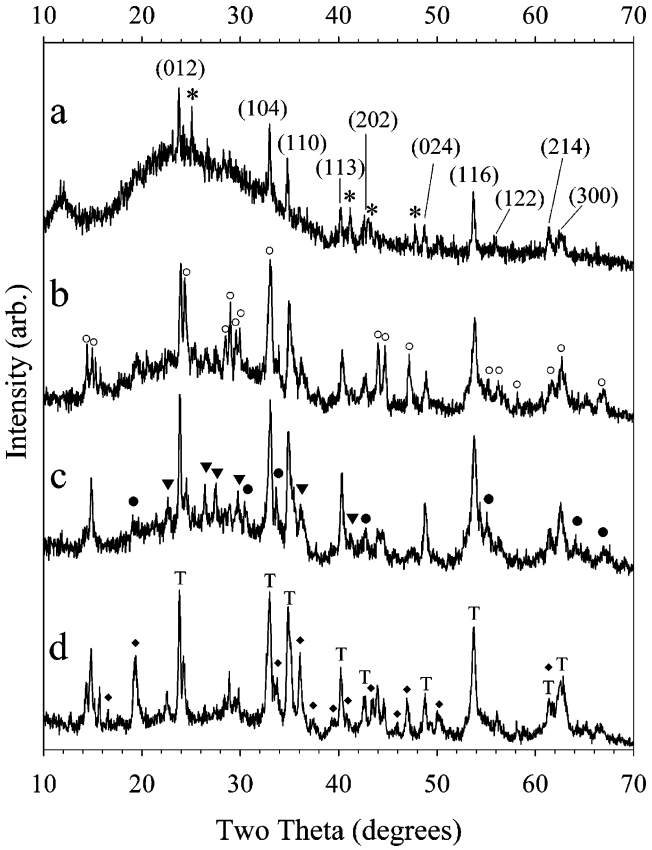

Figure 5. XRD stack plot of washed Ti_2O_3 products from $TiCl_3$ and $1.5Na_2O$ reactions (a) as-synthesized, synthesized with an additional (b) 5.3 mol of NaCl, (c) 7.9 mol of NaCl per mol of $TiCl_3$, and (d) the product of a $TiCl_3 + 1.62Na_2O + 5.3NaCl$ reaction. The (*hkl*) and T labels mark Ti_2O_3, * marks Ti_3O_5 (11-0217), ○ marks $Na_{0.23}TiO_2$, ● marks Ti_3O_5 (40-0806), ▼ marks Ti_6O_{11}, and ◆ marks $NaTi_2O_4$.

the reaction. Equation 3 theoretically should reach a T_{max} of 1465 °C, and because Ti_2O_3 has a melting point of 1842 °C, it is not surprising that the product is poorly crystallized. This reaction generated a similar product with and without the crucible insert with yields of 70−80% based on Ti_2O_3. The IR showed a broad Ti−O lattice vibration in the 470−520 cm^{-1} range. The black Ti_2O_3 product oxidizes to a white mixture of anatase and rutile TiO_2 upon heating in air at 500 °C. As expected, the black Ti_2O_3 powder (1.4 m^2/g) exhibits only modest MB photocatalysis relative to anatase-containing TiO_2 samples (∼25% degradation after 20 min of UV exposure, similar to rutile TiO_2).

Moderate sodium residues are still present in the acid-washed Ti_2O_3 product, which contains about 6.5 atom % Na relative to Ti (i.e., Na/Ti = 0.065). EDS also shows that chlorine residues are below detection limits. The sodium content is nearly double that seen in the TiO_2 products, and when the Ti_2O_3 sample is heated to 500−600 °C in a sealed evacuated ampule, the XRD pattern shows peaks consistent with $Na_{0.23}TiO_2$ (JCPDS no. 22-1404) in addition to Ti_2O_3, and the overall crystallinity is lower. The sodium is probably contained in an amorphous component that crystallizes or reacts with Ti_2O_3 upon annealing.

TG-DTA in flowing air shows that the Ti_2O_3 powder loses weight by 250 °C (∼0.7 wt %) likely due to adsorbed surface water and hydroxyl species and then gains weight during oxidation, which is complete by 950−1000 °C. The weight

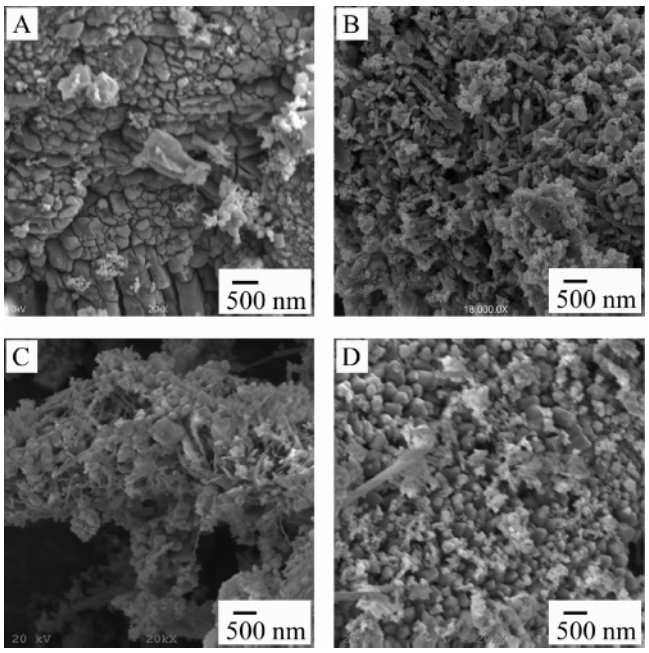

Figure 6. SEM of washed Ti_2O_3 products from $TiCl_3$ and $1.5Na_2O$ reactions (A) as-synthesized, (B) annealed at 600 °C in a vacuum, (C) synthesized with 5.3 mol of NaCl/mol of $TiCl_3$, and (D) synthesized with 7.9 mol of NaCl/mol of $TiCl_3$.

gain is ∼95% of that expected for an ideal Ti_2O_3 to TiO_2 oxidation. The product after 1000 °C TGA heating in air is primarily crystalline rutile TiO_2 (60 wt % Ti) with a trace of $Na_2Ti_6O_{13}$ ($Na_{0.33}TiO_{2.17}$). On the basis of a TiO_2 oxidation product, the observed oxidative weight gain translates to 63 wt % Ti in the starting sample. Ideally Ti_2O_3 has 67 wt % Ti, and the difference may be due to incomplete removal of surface residues from the wash process and the presence of an amorphous phase with Ti content lower than 67 wt % (e.g., $Na_{0.23}TiO_2$ is 56 wt % Ti).

NaCl and Excess Na_2O Additions to the Ti_2O_3 SSM Reaction. The hot SSM reaction may vaporize some of the titanium reagent out of the hot reaction zone, leaving excess Na_2O behind that could be the source of the excess sodium. Crucible containment and NaCl additions were again utilized to examine their effect on the progress of the Ti_2O_3 reaction. Two salt levels of 5.3 and 7.9 mol of NaCl/mol $TiCl_3$ were used, leading to reactions with T_{max} values of 875 °C and 801 °C (59% of NaCl is melted), respectively. The 5.3 mol NaCl addition leads to a more crystalline oxide mixture, comprised of primarily Ti_2O_3 and $Na_{0.23}TiO_2$ (Figure 5b). The 7.9 mol salt addition still contains these two phases, but with a much lower $Na_{0.23}TiO_2$ content and several peaks that probably correspond to Ti_6O_{11} ($TiO_{1.83}$, JCPDS no. 18-1401, Figure 5c). In an attempt to enhance formation of the $Na_{0.23}TiO_2$ phase, a crucible reaction with an NaCl:$TiCl_3$:Na_2O molar ratio of 5.3:1.0:1.62 was performed that has an ideal product formula of $Na_{0.24}TiO_{1.62}$, assuming no titanium loss during the reaction. This reaction produced a different mixture of phases, mainly Ti_2O_3, less $Na_{0.23}TiO_2$ than in Figure 5b, and the appearance of $NaTi_2O_4$ ($Na_{0.5}TiO_2$, JCPDS no. 45-0752, Figure 5d). When a higher excess amount of Na_2O was examined with a NaCl:$TiCl_3$:Na_2O molar ratio of 5.3:1.0:1.74, theoretically balanced for a $Na_{0.48}TiO_{1.74}$ product, the crystalline oxide lost most evidence for $Na_{0.23}TiO_2$

and has clear $NaTi_2O_4$ and Ti_2O_3 peaks with similar intensity. While the reactant ratio is difficult to control in these SSM reactions, other reagent choices may open up possibilities for a wide range of controllable alkali titanium oxide syntheses.

Morphology of Reduced Titanium Oxide Products. The morphology of the washed Ti_2O_3 product from $TiCl_3$ shows a heterogeneous aggregated mix of submicrometer particles that are generally between 50 and 500 nm (Figure 6A). Several of the particles show distinct hexagonal facets, consistent with the Ti_2O_3 unit cell structure. When this product is heated at 600 °C in an evacuated ampule and crystalline $Na_{0.23}TiO_2$ is detected, the SEM shows the appearance of rod- and particle-like shapes (Figure 6B), so the structural changes are reflected in morphological changes. The morphology also changes when NaCl is added in a crucible reaction as is shown in Figure 6C,D. The similarity between short rodlike nanostructures in Figure 6B,C suggests that the rod forms may be related to the presence of sodium containing products.

Conclusions

This study examined the effect of several modifications to the SSM reaction between solid $TiCl_3$ and Na_2O_2 that very rapidly and exothermically forms nanocrystalline TiO_2. Crucible containment and NaCl heat sink diluents were utilized to modify the crystalline phase and morphology of the resulting TiO_2. The overall particle size was adjusted from micrometer to sub-100 nm dimensions, while rutile crystallite sizes remained relatively unchanged (∼50−70 nm). The anatase phase content increased with NaCl additions, and its crystallite size was also fairly constant (∼30 nm). The SSM TiO_2 products with some anatase phase content have aqueous UV photocatalytic abilities that are comparable to or greater than a higher surface area commercial TiO_2 standard. It was also demonstrated that replacing Na_2O_2 with Na_2O as the solid oxygen source results in a poorly crystalline reduced Ti(III) oxide and black Ti_2O_3, as well as reduced Na−Ti−O phases, with some heat sink and reagent control over specific Na−Ti−O phase formation. This rapid SSM synthetic approach is amenable to systematic doping of the TiO_2 structure by strategies similar to those used in previous ZrO_2 phase stabilization studies.[18] Experiments along these lines are in progress, with the goal of improving anatase phase stability and enhancing visible light photocatalytic activity.

Acknowledgment. The authors thank the University of Iowa MPSFP grant program and the National Science Foundation (CHE-0407753) for partial funding support, R. B. Kaner (UCLA) for the suggestion of crucible use in SSM reactions, and K. Knagge (University of Iowa) for assistance with BET measurements.

CM0528328